Coping with Pleistocene climatic fluctuations: demographic responses in remote endemic reef fishes.

Erwan Delrieu-Trottin[1,2,3] | Nicolas Hubert[2] | Emily C. Giles[1,4] | Pascaline Chifflet-Belle[5,6] | Arnaud Suwalski[5,6] | Valentina Neglia[1] | Cristian Rapu-Edmunds[8] | Stefano Mona[5,6,7,†] | Pablo Saenz-Agudelo[1,†]

[1] Instituto de Ciencias Ambientales y Evolutivas, Universidad Austral de Chile, Valdivia, Chile

[2] Institut de Recherche pour le Développement, UMR 5554 (UM-CNRS-IRD-EPHE), ISEM, Montpellier, France.

[3] Museum für Naturkunde, Leibniz-Institut für Evolutions-und Biodiversitätsforschung an der Humboldt-Universität zu Berlin, Berlin, Germany

[4] Programa de Doctorado en Ciencias mención Ecología y Evolución, Escuela de Graduados, Facultad de Ciencias, Universidad Austral de Chile, Valdivia, Chile

[5] Institut de Systématique, Evolution, Biodiversité, ISYEB, Muséum national d'Histoire naturelle, CNRS, Sorbonne Université, EPHE, Université des Antilles, Paris, France

[6] EPHE, PSL Research University, Paris, France

[7] Laboratoire d'Excellence CORAIL, Papetoai, French Polynesia

[8] Mike Rapu Diving Center, Caleta Hanga Roa O'tai, Chile

†These authors jointly supervised this work.

Author for correspondence: Erwan Delrieu-Trottin,
e-mail: erwan.delrieu.trottin@gmail.com

Keywords: endemism, colonization, ddRADs, Easter Island, Rapa Nui, population genetics, genome wide sequencing

Abstract

Elucidating demographic history during the settlement of ecological communities is crucial for properly inferring the mechanisms that shape patterns of species diversity and their persistence through time. Here, we used genomic data and coalescent-based approaches to elucidate for the first time the demographic dynamics associated with the settlement by endemic reef fish fauna of one of the most remote peripheral islands of the Pacific Ocean, Rapa Nui (Easter Island). We compared the demographic history of nine endemic species in order to explore their demographic responses to Pleistocene climatic fluctuations. We found that Rapa Nui endemic species share a common demographic history as signatures of population expansions were retrieved for almost all of the species studied here, and synchronous demographic expansions initiated during the last glacial period were recovered for more than half of the studied species. These results suggest that eustatic fluctuations associated with Milankovitch cycles have played a central role in species demographic histories and in the final stage of the community assembly of many Rapa Nui reef fishes. Specifically, sea level low stands resulted in the maximum reef habitat extension for Rapa Nui endemic species; we discuss the potential role of seamounts in allowing endemic species to cope with Pleistocene climatic fluctuations, and we highlight the importance of local historical processes over regional ones. Overall, our results shed light on the mechanisms by which endemism arises and is maintained in peripheral reef fish fauna.

1 | INTRODUCTION

Demographic expansions are required to colonize novel environments and to establish new populations. Tracking the direction (expansions or contractions) and the magnitude of demographic changes through time can help elucidate not only when populations were established, but also reveal the factors that triggered such changes. For instance, if abiotic factors determined population sizes, we would expect to see populations expand or contract as environment changes. In contrast, population sizes should remain constant or decoupled from environmental changes when adaptation to new conditions is possible (Jump & Penuelas, 2005; Vrba, 1992; Wong & Candolin, 2015). Populations of different species can vary in their abilities to colonize novel environments and in the way that they cope with environmental variability (Hewitt, 2001, 2004; Lessa, Cook, & Patton, 2003). The degree to which colonization dynamics and/or responses to environmental changes are synchronous have not been well-characterized. Overall, uncovering patterns acting at multispecies levels is crucial to understanding how climatic fluctuations can ultimately drive patterns of community assembly and thus the distribution of current biodiversity (Chan, Schanzenbach, & Hickerson, 2014).

Colonization dynamics and responses to climatic fluctuations can leave a detectable genetic footprint of changes in population size (Wakeley, 2009, 2010). A large number of studies have shown that past major climatic fluctuations, with expansions and contractions of ice sheets and sea level fluctuations (Cutler et al., 2003; Pahnke, Zahn, Elderfield, & Schulz, 2003) have indeed deeply impacted the demography of many terrestrial and marine species (Avise, 2009; Hewitt, 2003; Hickerson et al., 2010; Petit et al., 2003). Theory predicts that assemblages of co-distributed species with similar physiological and habitat requirements should respond similarly to environmental changes (Hewitt, 2001, 2004b; Lessa, Cook, & Patton, 2003). In the same manner, assemblages of co-distributed species of similar ages should display similar colonization timings and dynamics, as well as concerted changes in their population sizes through time. Synchronicity of population size changes of co-distributed taxa has only been recovered a few times in terrestrial and marine environments (e.g. Burbrink et al., 2016; Chan et al., 2014; Reid, Naro-Maciel, Hahn, FitzSimmons, & Gehara, 2019).

Coral reefs are among the most diverse ecosystems, yet how this biodiversity has arisen and is maintained remains largely debated. Among coral reef organisms, coral reef fishes represent the most diverse and widely distributed group of vertebrates on the planet (Nelson, Grande, & Wilson, 2016). Their geographic distribution is uneven; in particular, endemism hotspots, i.e. regions hosting high proportions of species with geographically restricted distributions, are found along the periphery of the Indo-Australian Archipelago (Allen, 2008; Bellwood & Wainwright, 2002; Delrieu-Trottin et al., 2015; Eschmeyer, Fricke, Fong, & Polack, 2010; Gaboriau, Leprieur, Mouillot, & Hubert, 2018; Hughes, Bellwood, & Connolly, 2002; Randall, 2005, 2007; Randall & Cea, 2011). As such, a series of questions remain unanswered regarding the mechanisms enabling the co-existence of hundreds of species locally and the existence of large diversity gradients in the Indo-Pacific (Allen & Erdmann, 2012). Reconstructing the demographic histories of populations in these hotspots of endemism could provide key information on how coral reef fish biodiversity is maintained in coral reef ecosystems.

Rapa Nui (Chile, 166 km2) is the most remote peripheral hotspot of endemism of reef fishes; it is composed of 21.7% endemic species and includes all major reef fish families and a high diversity of life history traits (Cea, 2016; Randall & Cea, 2011). Despite being the second, after Hawai'i (Randall, 1998, 2007), hotspot of endemism for reef fishes in the tropical Indo-Pacific, the mechanisms that have underlined the persistence of species with such range-restricted distributions through geological time remain enigmatic. The Rapa Nui reef fish community is not only exceptional for its high percentage of endemic species, but also for being extremely species-poor for a tropical reef system (only 169 fish species; 139 shore fishes) By comparison, the Indo-Australian Archipelago houses more than 2,600 reef fish species (Allen & Erdmann, 2012). Rapa Nui and the islet Motu Motiro Hiva (Salas y Gómez, 0.15 km2), located 400 km further east and which shares the same reef fish fauna as Rapa Nui (Friedlander et al., 2013), constitute the only two emerged islands of the Easter Chain. Rapa Nui and Motu Motiro Hiva are relatively young; 2.5 and 1.7 My, respectively (Clouard & Bonneville, 2005), but they are embedded in a network of numerous seamounts. This seamount chain extends 2,232 km east to the Nazca seamount (23°360 S, 83°300 W) (Clouard & Bonneville, 2005; Ray et al., 2012) and these mounts

114 have emerged to various degree during periods of low sea level. In this context, an
115 "Ancient Archipelago" hypothesis has been formulated by Newman & Foster (1983) to
116 account for the high level of endemism observed in Rapa Nui and Motu Motiro Hiva
117 that further questions the dynamics of community assembly in such a remote system.
118 This hypothesis states that seamounts could have provided potentially suitable habitat
119 for the past 29 My during periods of low sea level (lowstands) for endemics of the
120 region, allowing them to evolve and persist up to present times (Newman & Foster,
121 1983). Interestingly, a recent analysis of the divergence times of endemic species from
122 their closest relatives indicates that most species endemic to Rapa Nui are
123 neoendemics, i.e. younger than the emergence of Rapa Nui and Motu Motiro Hiva
124 (Delrieu-Trottin et al., 2019).

125 Seamounts near Rapa Nui could have played a major role in species
126 persistence through time, especially during the sea-level fluctuations of the Pleistocene
127 that resulted in changes of up to 150 m below present levels (Miller et al., 2005). This
128 hypothesis is increasingly called to attention as recent surveys showed that many
129 Rapa Nui endemic species can be found from shallow waters to the mesophotic zone
130 (at least 160 m) in Rapa Nui waters and in nearby seamounts (Easton et al., 2017).
131 The paleo-environmental perturbations of the Pleistocene might be expected to have
132 left a footprint on the community assembly and the associated demographic histories
133 of these populations (Bard et al., 1996; Delrieu-Trottin et al., 2017; Hewitt, 2004; Ludt
134 & Rocha, 2015; Woodroffe et al., 2010). For instance, numerous species are reported
135 as present in Rapa Nui waters but are actually vagrants, i.e. species that colonize Rapa
136 Nui from time to time without being able to establish a stable population locally (Randall
137 & Cea, 2011), suggesting the current isolated state of Rapa Nui is not well-suited for
138 species immigration compared to lowstands. Reconstructing the demographic
139 histories of populations in this hotspot of endemism could provide key information on
140 how endemic species cope with Pleistocene climatic fluctuations.

141 The present study investigates the demographic history of multiple species of
142 coral reef fishes in Rapa Nui possessing distinct range sizes and life-history traits. We
143 used genome-wide sequencing (ddRAD) and coalescent-based approaches in order
144 to highlight potential demographic trends during community assembly. We hypothesize
145 that sea-level fluctuations have left different signatures on the demographic history of

Rapa Nui reef fish species, and these depend on specific characteristics of species. In particular, (1) we expect that species with large range distributions have functioned as a metapopulation and that this metapopulation dynamics have mitigated the impacts of sea level fluctuations on their demographic histories, (2) fish species restricted to shallow waters should have more frequent fluctuations of population sizes; thus, wider occurrence along a depth gradient could mitigate the impact of sea level fluctuations. Lastly (3) signals of population growth in Rapa Nui endemic fishes should have occurred during low stands. This is expected as a corollary of the Ancient Archipelago hypothesis where the higher number of emerged seamounts around Rapa Nui should have favored population expansions. To our knowledge, this represents the first attempt to reconstruct the demographic history of an assemblage of endemic coral reef fishes of one of the least studied coral reef communities of the Indo-Pacific Ocean.

2 | MATERIALS AND METHODS

2.1 | Sampling

Rapa Nui hosts two types of endemic species, small-range and large-range endemic species. Small-range endemics are only present around Rapa Nui and Motu Motiro Hiva and have a maximum range of <500 km in linear distance, see Delrieu-Trottin, Maynard, & Planes (2014). Southern subtropical endemics have large-ranges (1,000–8,000 km in linear distance, see Delrieu-Trottin et al. (2014), hereafter large-range endemic species) and are distributed from Southern Polynesia to Rapa Nui (regional endemics in Friedlander et al. (2013)). Large-range endemics, contrary to small-range endemics, are present both in Rapa Nui and in other southern subtropical islands of the Pacific. As such, populations of these fishes are embedded in metapopulations of larger geographic ranges than those of small-range endemics, making them potentially prone to not only processes at the scale of Rapa Nui (local processes) but also at the scale of the South Pacific (regional processes). A total of 143 reef fishes, belonging to nine species, were collected using polespears or an anesthetic (clove oil) in Rapa Nui in October 2016 (**TABLE 1**). The fishes collected represent the two types of endemics (small-range endemics: 7 species; large-range endemics: 2 species). The species analyzed here belong to seven major reef fish families and possess different reproductive strategies, with five species producing pelagic eggs, three species

178 producing demersal eggs, and one species brooding eggs in their mouths (**TABLE 1**).
179 Overall, we investigated the consequences of historical processes, such as sea level
180 changes, and ecological dynamics, i.e. those driven by reproductive strategy, on the
181 observed genetic diversity. If historical processes were more important than ecological
182 processes in the maintenance of endemic species in Rapa Nui, we would expect to
183 find similar population dynamics for the two types of endemic species.
184

185 **2.2 | Library preparation and sequencing**

186 Whole genomic DNA was extracted from fin or gill tissue preserved in 96% ethanol
187 using the GeneJet Genomic DNA purification kit according to the manufacturer's
188 protocols (Thermo Fisher Scientific). Double-digest restriction-associated DNA
189 (ddRAD) libraries were prepared following Peterson et al.' (2012) using EcoRI and
190 MspI restriction enzymes, a 400 bp size selection and a combination of two indexes
191 and 24 barcodes to pool 48 individuals per lane. The genomic libraries obtained were
192 sequenced in three lanes of a HiSeq 2500 Illumina sequencer (single end, 125 bp).
193 Illumina reads are available from the Sequence Read Archive (SRA) at NCBI under
194 the BioProject Accession no: PRJNA622670.
195

196 **2.3 | De novo assembly and SNP calling**

197 We used the 'process_radtags.pl' pipeline in STACKS version 2.0 (Catchen,
198 Hohenlohe, Bassham, Amores, & Cresko, 2013; Catchen, Amores, Hohenlohe,
199 Cresko, & Postlethwait, 2011) to demultiplex and quality filter the sequences obtained.
200 In the absence of reference genomes for the species under study, RADSeq loci were
201 assembled de novo using the 'denovo_map.pl' pipeline in STACKS each species
202 separately. We used the parameter combination recommended by Mastretta-Yanes et
203 al. (2015); this included minimum read depth to create a stack (m) = 3, number of
204 mismatches allowed between loci within individuals (M) = 3, number of mismatches
205 allowed between loci within catalogue (n) = 3 and required a locus to be present in all
206 individuals of each species (r = 1). Following de novo mapping, an initial data-filtering
207 step was performed using the population component of STACKS removing all loci with
208 maximum observed heterozygosity higher than 0.8. We kept all single-nucleotide
209 polymorphisms (SNP) per stack (i.e. locus) and did not use any threshold regarding

the minor allele frequencies as these rare variants are informative when performing demographic inference (Wakeley, 2009). We then removed all loci displaying more than three SNPs to avoid potential paralogues. Heterozygosity (H), FIS, mean pairwise differences (π) computed on all sites of variable loci and Watterson's theta (Θ_w) computed on all sites of variable loci were calculated in R (R Core Team, 2017) using the packages vcfR (Knaus & Grünwald, 2017), adegenet (Jombart, 2008; Jombart & Ahmed, 2011), PopGenome (Pfeifer, Wittelsbürger, Ramos-Onsins, & Lercher, 2014) and pegas (Paradis, 2010).

2.4 | Statistical analyses of genetic diversity indices and reconstruction of potential habitats given present and past sea level conditions

We tested whether the summary statistics (Θ_w, π, He), neutrality tests (Tajima's D and Fu and Li's D) and TMRCA obtained for each species were related to range size (small-range / large-range endemics), and/or reproductive strategies (pelagic eggs / demersal eggs / mouth brooding). We used a multivariate regression tree (MRT) (De'ath, 2002) on normalized summary statistics to hierarchize the significant predictor variables. Prediction error was used to assess model fit and determine the appropriate tree size, and the tree was pruned by cross-validation using the minimum rule (Breiman, Friedman, Olshen, & Stone, 1984). All statistical analyses were performed in R, using the packages vegan (Oksanen et al., 2012) and mvpart (Therneau, Oksanen, Oksanen, Atkinson, & De'ath, 2014) while graphical representations were performed using ggplot2 (Wickham, 2009).

Finally, as Rapa Nui and Motu Motiro Hiva are part of the Easter chain composed of numerous seamounts, we examined how eustatic changes modified the surface of potential habitat for Rapa Nui endemic species. We investigated whether periods corresponding to minimum sea level constituted an extension or a reduction of potential available habitat for Rapa Nui endemic fishes using the package marmap (Pante & Simon-Bouhet, 2013) in R. We reconstructed both present surface habitat using the maximum depth recorded for all species (160 m) and surface habitat given the scenario of a minimum sea level (sea level lowstand, -120 m context), corresponding to the surface between -120 and -280 m depth.

242 **2.5 | Demographic inferences**

243 To detect departures from the neutral Wright–Fisher model, we computed Tajima's D
244 and Fu & Li's D neutrality tests implemented in PopGenome. Significance of Tajima's
245 D (TD) was evaluated after 1000 coalescent simulations of a constant population
246 model with size Θ_w using fastsimcoal and a custom script. Significant negative values
247 of these tests indicate population growth while significant positive values are a
248 signature of either genetic subdivision or population contraction assuming selective
249 neutrality. The folded Site (Allele) Frequency Spectrum (SFS), describing the
250 distribution of allele frequencies across polymorphic sites, was computed in R with the
251 package pegas (Paradis, 2010). The SFS represents a summary of genetic variation
252 whose shape is sensitive to underlying population genetic processes (population size
253 change, migration, selection, etc.). The aggregated SFS (aSFS, Xue & Hickerson,
254 2015) was then computed using a custom R script. The aSFS combines an array of
255 independent SFSs computed in each species into a single SFS vector. First, the
256 independent SFSs need to have the same number of classes (i.e., each species must
257 have the same number of individuals). To this end, we downsampled all SFSs to 13
258 diploid individuals, the minimum sample size in our nine species. Each SFS was then
259 transformed into a proportion vector by dividing each class by the total number of
260 SNPs. We then arranged the nine bins within each frequency class in descending order
261 of proportion of total SNPs. The ordering is therefore independent in each frequency
262 class, so that there is no relationship between the initial order of the single taxon and
263 the resulting aSFS, which guarantees exchangeability across single taxon SFSs. The
264 final vector contains a number of classes equal to the number of species times the
265 number of frequency classes (i.e., 9 x 13 in our case).

266 Demographic inferences were investigated reconstructing the variation in the
267 effective population size (Ne) through time using three independent approaches. First
268 we ran the composite likelihood approach implemented in the software stairwayplot
269 (Liu & Fu, 2015). The *stairwayplot* is a non-parametric model where Ne is free to vary
270 at each coalescent interval. The composite likelihood is evaluated as the difference
271 between the observed SFS and its expectation under a specific demographic history.

272 Second, we ran an approximate Bayesian computation algorithm based on
273 coalescent simulations following Maisano Delser et al (2016) to compare the results

obtained by the *stairwayplot*. Briefly, we performed 1,000,000 coalescent simulations of a demographic model with three instantaneous changes of Ne. This number was chosen as a compromise between over parametrization and the need to capture multiple demographic changes through time. We further ran a simplified model with only one instantaneous size change to determine if its use in the hierarchical ABC analysis (hABC, see below) would have failed to detect important historical events and biased the results. The full model is therefore defined by seven parameters: four values of Ne and three instantaneous time changes (hereafter, T). We set the same prior uniform distribution for the four Ne values and incremental uniform distribution for the three T parameters, similarly to Maisano Delser et al. (2016). The simplified model is defined by three parameters: two values of Ne and one instantaneous size change. The two models provided similar results and we therefore used the simplified one in the hABC. Coalescent simulations and SFS computation were performed with fastsimcoal (Excoffier, Dupanloup, Huerta-Sánchez, Sousa, & Foll, 2013a). We used the SFS and the mean pairwise differences (π) as summary statistics. We retained the best 5,000 simulations to perform a local linear regression (Beaumont, Zhang, & Balding, 2002) and reconstructed the abc skyline at user specified time points as in Maisano Delser et al. (2016).

Third, we performed a hierarchical approximate Bayesian computation (hABC) analysis with the goal of detecting potential concerted demographic histories across the species under study (Chan et al., 2014). This method allows combining the datasets from the nine species investigated here into a single analysis in order to estimate objectively when population size changes occurred, whether they were synchronous, and the timing of such demographic changes (Burbrink et al., 2016; Chan et al., 2014). We first extracted the number of species ζ with synchronous changes in effective population size from a uniform prior distribution bounded between 1 and n (total number of species). We then extracted the time of co-change (τ_s) and attributed this to ζ randomly chosen species. If $\zeta < n$, the remaining times were independently extracted from the same prior used for τ_s. We then computed $E(\tau)$, the average over the n times of change, and the dispersion index computed as the ratio between the variance of these times and $E(\tau)$ (Chan et al., 214). Each species follows a simple model of instantaneous size change with two Ne (modern and ancestral)

306 extracted from independent prior distributions (i.e., two priors for each species). We
307 defined the same priors for both Ne to avoid weighting expansions or contractions *a*
308 *priori*. The rationale here is that some species could have started expanding while
309 others were contracting at the same time (for example, species adapted to cold climate
310 will contract when species adapt to warmer weather will expand, having synchronous
311 though opposite responses). We also took species specific generation times into
312 account when running the simulations. We first performed hABC on the nine species
313 and then restricted the analysis to the species displaying the most similar demographic
314 profiles (see Results). We performed 2,000,000 coalescent simulations with
315 fastsimcoal (Excoffier et al., 2013a) and computed summary statistics (aSFS, mean
316 and standard deviation over species of Θ estimated from singleton, Π, and TD) with a
317 custom R script. Local linear regression was finally applied to the best 5,000
318 simulations to estimate the posterior distribution of each parameter. We performed a
319 cross validation experiment to determine whether we could correctly infer ζ given our
320 settings (number of species, loci and summary statistics) by randomly sampling 1,000
321 datasets generated from prior distributions and re-analyzed them under the same
322 hABC conditions. Finally, a posterior predictive test was run by sampling 50,000
323 random combinations of parameter values from the hABC posterior distributions with
324 which we simulated pseudo-observed datasets (Bertorelle et al. 2010). A principal
325 component analysis was then applied to check if the estimated model could reproduce
326 the observed data by comparing the aSFS computed using the pseudo-observed and
327 the observed data.

328 Uncertainty in both mutation rates and generation times can potentially bias
329 molecular dating. Estimated mutation rates for SNP data of fish range from 2.5×10^{-8}
330 (Kavembe, Kautt, Machado-Schiaffino, & Meyer, 2016) to 3.5×10^{-9} (Malinsky et al.,
331 2018) and their selection for estimating demographic histories is not often justified. As
332 such, for all analysis here we chose the hypothesized fish SNP mutation rate (μ) most
333 often used in the literature; 1.0×10^{-8} / site / generation (Jacobs, Hughes, Robinson,
334 Adams, & Elmer, 2018; Le Moan, Gagnaire, & Bonhomme, 2016; Rougeux,
335 Bernatchez, & Gagnaire, 2017; Souissi, Bonhomme, Manchado, Bahri-Sfar, &
336 Gagnaire, 2018; Tine et al., 2014). Estimations of generation times in the wild for fishes
337 are scarce. Most of the generation times we used (six out of nine) were selected from

338 the literature from species that are phylogenetically closely-related to the species
339 studied here (same genus) (**TABLE 1**). Alternatively, we inferred generation time using
340 maximum standard length (three species), as maximum standard length and
341 generation time are positively correlated (Froese & Binohlan, 2000).
342
343 **3 | RESULTS**
344 **3.1 | Raw sequence filtering, assembly, and SNP calling.**
345 A total of 499,403,262 reads were obtained for the 143 individual samples from the
346 nine species endemic to Rapa Nui. The different filtering steps resulted in the building
347 of an average of 41,470 RAD loci of 120 bp per species (min: 25,331 loci (*Chrysiptera*
348 *rapanui*); max: 63,590 loci (*Ostorhinchus chalcius*)) out of which an average of 23,693
349 loci were variable. *Myripristis tiki* displayed the highest number of variable RAD seq
350 loci (28,855) while *Chrysiptera rapanui* had the lowest (19,246) (**TABLE 2**).
351 *Chrysiptera rapanui* displayed the highest percentage of variable RAD seq loci (76%)
352 while *Ostorhinchus chalcius* displays the lowest (38%). The variable RAD loci harbored
353 an average of 37,107 SNPs (min: 28,239 (*Cantherhines rapanui*); max: 46,718
354 (*Myripristis tiki*)). The depth of coverage per SNP ranged from 31x to 50x (43x
355 averaged across species).
356
357 **3.2 | Population genetic statistics**
358 A summary of the principal statistics is presented in **TABLE 2**. Briefly, the observed
359 heterozygosity values varied from 0.137 ± 0.018 (*Chrysiptera rapanui*) to 0.262 ± 0.032
360 (*Cantherhines rapanui*) and no departures were observed when compared to expected
361 heterozygosity. The FIS values were overall very low for all species, ranging from 0.008
362 (*Ostorhinchus chalcius*) to 0.043 (*Chromis randalli*). Watterson's theta values
363 computed on all sites of variable loci ranged from 26.61 x 10^{-4} (*O. chalcius*) to 37.65 x
364 10^{-4} (*Centropyge hotumatua*) while π computed on all sites of variable loci varied more
365 extensively, from 18.65 x 10^{-4} (*O. chalcius*) to 31.63 x 10^{-4} (*Cantherhines rapanui*). All
366 Tajima's D values were significant (**TABLE 2**). *Cantherhines rapanui* displayed the
367 only positive value, suggesting a population contraction (bottleneck), while the
368 remaining eight species displayed negative values, suggesting population growth.

We found that none of these population genetic statistics were correlated with other factors such as family, demography, range-size classification, reproductive strategy, or generation time after an MRT analysis. The two-leaf MRT for normalized π, Θ_w, Ho, Tajima's D and Fu & Li's D explained a high proportion of total variance (67.9%, **FIGURE 1A**) and divided the dataset into two clusters: the first cluster (Cluster 1) was composed of both large range and small range endemics, included all types of reproductive strategies and the lowest π, Θ_w, Ho, Tajima's D and Fu & Li's D values (*Centropyge hotumatua, Ostorhinchus chalcius, Chrysiptera rapanui, Chromis randalli, Myripristis tiki*). Conversely, the second cluster (Cluster 2) displayed the highest values for all summary statistics (*Sargocentron wilhelmi, Cantherhines rapanui, Chaetodon litus, Coris debueni*). This result was confirmed by visual inspection of the SFS, with species of the first cluster displaying a spectrum fitting a clear expansion while species of the second cluster displayed a spectrum supporting either a bottleneck (*Cantherhines rapanui*) or weak expansion (*Chaetodon litus*, *Coris debueni* and *Sargocentron wilhelmi*) (**FIGURE 1B**).

3.3 | Changes in historical effective population size

As both *stairwayplots* and the abc skylines were used to compute changes in effective population sizes, we chose to consider only changes in Ne observed with both methods. We recovered concordant signals with the two methods, with signatures of population expansions for eight out of the nine species and signature of a bottleneck for only one species (**FIGURE 2, 3**). Expansion times retrieved were highly similar between the two methods for most species in Cluster 1: *Centropyge hotumatua* (ca 75,000 ypb); *Chromis randalli* (ca 100,000 ypb); *Chrysiptera rapanui* (ca 50,000 ypb); *Myripristis tiki* (ca 130,000 ypb), but differed for *Ostorhinchus chalcius* (20,000 (stairway) vs 125,000 (abc) ypb). For Cluster 2, abc skylines dated older demographic events for the bottleneck retrieved in *Cantherhines rapanui* (22,000 (stairway) vs 50,000 (abc) ypb) and for the older expansion times retrieved in *Chaetodon litus* (40,000 (stairway) vs 200,000 (abc) ypb), and *Coris debueni* (140,000 (stairway) vs 250,000 (abc) ypb); *Sargocentron wilhelmi* (180,000 (stairway) vs 380,000 (abc) ypb)) (**FIGURE 2, 3**).

The hABC analyses allowed us to test the synchronicity of the observed changes in Ne. The estimate for ζ was consistent with a concerted expansion for most species, as the median of the ζ posterior distribution obtained was 6 (**FIGURE 4**). Cross-validation suggested that the median is the best point estimate for ζ (**FIGURE S2**), while the mode did not perform well, with most datasets displaying 1 or 9 no matter the real value of ζ. We retrieved a co-expansion time of 154,200 ypb (97.5% CI: 64,687 - 339,057 ypb) and an older mean time ($E(\tau)$ = 187,437 ypb, 97.5% CI: 156,140 - 239,756). Restricting the analysis to the species displaying the clear expansions (species of Cluster 1), we found a stronger and younger pulse of coexpansion (τ_s = 45,836 ypb, 97.5%, CI: 30,023-87,767 ypb) associated with a younger mean expansion time ($E(\tau)$: 82,471 ypb , 97.5% CI: 69,691-107,510 ypb) (**FIGURE 4**). The posterior predictive test highlighted that the estimated model could reproduce the observed data, as shown by the PCA computed on the aSFS of the pseudo-observed and observed data (**FIGURE S3**). The mean TMRCA retrieved with the *stairwayplots* for the nine species was very recent 253,871 ypb (+/- 119,482 ypb) and ranged from 105,232 ypb (*Ostorhinchus chalcius*) to 398,058 ypb (*Sargocentron wilhelmi*) (**FIGURE 1**). Including normalized TMRCAs in the previous MRT analyses resulted in the formation of the same two partitions, with species of Cluster 1 having younger TMRCAs than species of Cluster 2 (65.6% of variance explained, **FIGURE S1**).

Overall, we recovered three different demographic patterns, concordant with the aSFS profiles and the neutrality tests obtained. (a) The five species of Cluster 1 displayed high magnitude population expansions, with modern Ne being on average 11.8 times higher than the corresponding ancient Ne. (b) Older and weaker expansions were found for two species (*Coris debueni, Chaetodon litus*, *Sargocentron wilhelmi*), with modern Ne being on average 2.8 times higher than their ancient Ne. (c) Lastly, a bottleneck was found for *Cantherhines rapanui*, with modern Ne 1.6 times lower than the ancient Ne.

3.4 | Reconstruction of the surface of potential habitat

Reconstruction of the potential present and past habitat during periods of low sea level conditions (-120 m) showed that rise in sea level resulted in a reduction of 38.6% of the potential habitat (**FIGURE 5**). This reduction in potential habitat was accompanied

by a reduction in the number of potential seamounts colonized, from 18 to 11 (**FIGURE 5**). It is worth noting that the Apollo seamount was not recovered as a present nor a past habitat despite the fact that the species *Sargocentron wilhelmi* and *Chaetodon litus* have been observed there recently (**TABLE 1**); the resolution of the depth gradient might be the cause of this discrepancy.

4 | DISCUSSION

4.1 Genetic diversity and demographic changes - identifying common patterns among species

Identifying general patterns in ecosystems is of fundamental importance to understand species responses to environmental changes and underlying eco-evolutionary dynamics. Studies combining multiple species in joint demographic analyses at the community-scale are still scarce in the literature, but they will progressively shed light on common past demographic changes and eventually help to predict future dynamics. Here we harnessed the power of population genomics to uncover the historical demography of one of the most remote coral fish assemblage of the Pacific Ocean. To detect the co-occurrence of similar demographic responses, we first inspected the genetic variability of the nine species and then inferred their demographic history individually through coalescent-based analyses. Overall, we found that Rapa Nui endemic species share a common history, with population expansions dominating the demographic histories of eight out of the nine species studied here. We found signatures of demographic changes that could be dated for most of the species to the last glacial period for both small-range and large-range endemics. We identified one cluster of five species showing a strikingly similar pattern of population expansions (Cluster 1), and a second cluster composed of mildly expanding populations and one species (*Cantherhines rapanui*) experiencing a contraction (**FIGURE 1,2,3; TABLE 2**). We quantitatively confirmed this result using an hABC model, which found a group of six co-varying species dated at 154,200 ybp (97.5% CI: 64,687 - 339,057 ypb; **FIGURE 4**). The hABC requires, however, a larger number of species to be included in the analysis in order to detect synchronous changes in effective population size (Chan et al. 2014), and our results of cross validation suggest that even with genomic data there is some uncertainty regarding the exact number of co-varying species (**FIGURE S2**).

Combining all of the descriptive and inferential evidences, we therefore ran the hABC analysis on Cluster 1 only to refine the estimation of the timing of co-expansion. A stronger and younger signal of co-variation has been retrieved and dated the coexpansion at 45,836 ypb (97.5%, CI: 30,023-87,767 ypb; **FIGURE 4**), confirming the presence of two clusters among expanding species.

4.2 | Imprint of sea-level fluctuations on the demographic history of Rapa Nui reef fish species

Sea level oscillations over the past 800,000 years (Augustin et al., 2004; McManus, 2004) and particularly during the Last Glacial Maximum (LGM, from 19,000–20,000 to 26,500 years ago, Clark et al. (2009)) have been hypothesized as greatly affecting coral reef fish populations as coral reef fish species commonly studied are restricted to shallow waters (0-30 m depth, Craig, Eble, & Bowen, 2010; Craig, Eble, Bowen, & Robertson, 2007; Crandall, Frey, Grosberg, & Barber, 2008; Fauvelot, Bernardi, & Planes, 2003; Gaither, Toonen, Robertson, Planes, & Bowen, 2010; Hellberg, 2001; Horne, van Herwerden, Choat, & Robertson, 2008; Klanten, Choat, & Van Herwerden, 2007; Robertson, 2004; Winters, van Herwerden, Choat, & Robertson, 2010). Rapa Nui endemics, however, differ in their ecology compared to organisms of other reefs in the Pacific region, as they seem far less restricted in terms of habitat and depth range. Many of the Rapa Nui endemic species have the particularity of being found from shallow waters to the mesophotic zone, down to at least 160 m in Rapa Nui waters and in nearby seamounts (**TABLE 1**). Considering the network of seamounts surrounding Rapa Nui, low sea levels would have produced periods of maximum reef habitat extension for Rapa Nui endemic species. As such, population expansions observed for most species during the glacial period, a period characterized by climatic cooling and decreased sea level, could reflect the colonization / recolonization history of Rapa Nui from Motu Motiro Hiva or other seamounts of the Rapa Nui archipelago. While the Ancient Archipelago hypothesis of Newman & Foster (1983) has been invalidated at the species level for this island system (Delrieu-Trottin et al., 2019), this hypothesis could explain what is observed at the population level for most Rapa Nui endemic species (i.e. a recolonization from the seamounts rather than from elsewhere in the Pacific).

We would expect to recover a recent bottleneck for all species following sea level rise and corresponding reduction of habitat, a bottleneck correlated with the LGM (Fauvelot et al., 2003; Ludt & Rocha, 2015) was only observed for *Cantherhines rapanui.* This species, together with the apogonid *Ostorhinchus chalcius*, possesses one of the most restricted depth ranges among the species studied here (0-20m, see **TABLE 1**). However, it is important to note that *O. chalcius* is a nocturnal predator and is cryptic during the day. Therefore, it is highly likely that its current depth range is an underestimation that is limited to technical constraints of mesophotic fish surveys. As such, this assumption could explain to some extent why we did not find signal of a bottleneck for this species. In contrast, the restricted depth range of *Cantherines rapanui* could be the reason why the demographic pattern of this species differs from that of the other studied species. More specifically, a restricted depth range would have made this species more vulnerable to sea level fluctuations during the LGM compared to the other Rapa Nui endemics. The ability to thrive across a large depth gradient might have buffered the influence of the LGM on most Rapa Nui endemic populations. Mesophotic reefs usually host different communities of species (Rocha et al., 2018), a change that is attributed to either competition and/or adaptation to such habitats. The low species diversity in Rapa Nui might be one of the factors influencing the presence of Rapa Nui endemics with the capability of inhabiting such large depth gradients.

4.3 | Community assembly in remote islands – importance of local processes

The common demographic and temporal patterns found for both large-range and small-range endemics also provide insights into the mechanisms that shaped the Rapa Nui ichthyofauna. Community assembly in remote islands is expected to rely on colonization / extinction / recolonization processes. Populations of large-range endemics sampled around Rapa Nui could potentially operate at a regional scale. However, we observed concordant expansion times for species of Cluster 1 (*Centropyge hotumatua, Ostorhinchus chalcius, Chrysiptera rapanui, Chromis randalli, Myripristis tiki*) including two large range endemics, suggesting that population demographic histories have been driven by local historical processes and that neighboring populations have minimally affected the demography of these species.

528 This is consistent with the isolation of Rapa Nui, which is mirrored by its relatively lower
529 species richness compared to that of other Pacific islands. The low species diversity
530 in Rapa Nui reefs might be due not only to the difficulty of larvae to colonize such
531 remote islands, but also due to the difficulty of establishing a viable population /
532 metapopulation that functions at such local scales. This hypothesis is reinforced by the
533 fact that the two large range endemics studied here are among the most abundant
534 species of Rapa Nui (Friedlander et al., 2013), yet they are rare throughout the rest of
535 their distribution (Randall, 2005). Assessing the amount of gene flow between Rapa
536 Nui populations with those of Pitcairn or Austral Island for these large range endemics
537 could help to test this hypothesis. The predominance of local over regional processes
538 on the population demography of remote endemic species has also been reported for
539 Marquesan endemic reef fish species (Delrieu-Trottin et al., 2017) and for species
540 endemic to the oceanic islands of the Vitória–Trindade Chain (Pinheiro et al., 2017),
541 arguing in favor of potentially common processes for peripheral hotspots of endemism.
542

543 **4.4 | Limitations of the demographic inferences**

544 We reconstructed the demographic history of the Rapa Nui fauna following three
545 independent approaches that have complementary strengths and shortcomings in
546 estimating both the direction, the magnitude and the timing of demographic changes
547 through time. The *stairwayplot* is a “model-flexible” (or model-free) approach similar to
548 skyline plot approaches (Drummond, Rambaut, Shapiro, & Pybus, 2005; Drummond
549 & Rambaut, 2007; Heled & Drummond, 2008; Pybus, Rambaut, & Harvey, 2000). Not
550 restricted to a specific demographic model, Ne is free to vary at each coalescent
551 interval, allowing the exploration of a large model space (Liu & Fu, 2015). The large
552 number of Ne parameters may result difficult to estimate when the SNPs panel is
553 relatively small (Lapierre, Lambert, & Achaz, 2017). Moreover, we are specifically
554 interested in the time when a change in Ne occurred, which is only indirectly estimated
555 by the *stairwayplot* as a function of the changes in Ne. On the other hand, the
556 Approximate Bayesian Computation (ABC) framework explicitly modeled three-time
557 parameters while the variation of Ne through time is reconstructed a posteriori
558 (Maisano Delser et al., 2016), having the drawback of approximating the likelihood of
559 the data using summary statistics. For these reasons, *stairwayplot* and the abc skyline

560 are highly complementary and it is important to run both of them to gain a robust insight
561 into species demography. The discrepancy we observed in the timing of change
562 between the two approaches, but not in the trend, it is clearly related to the large
563 variance associated with the estimation process. More genomic data or more species
564 are needed to minimize this variance and the differences observed between the
565 *stairwayplot* and abc skyline results. Here we combined more species using the hABC
566 approach to quantitatively test the synchronicity of the changes in Ne (Chan et al.,
567 2014). The hABC approach is necessarily limited by an a priori choice of the
568 demographic models characterizing the species under investigation. Here we adopted
569 a simple three parameters model because all previous analyses on single species
570 have suggested it could be enough to describe the dynamics of Ne through time.
571 Overall, the addition of more species to these analyses as the power to correctly infer
572 the number of co-varying species increases for larger datasets (Chan et al., 2014).
573 Finally, the selection of the mutation rates and generation times can greatly
574 impact the timing and the magnitude of the demographic estimates. During the last 20
575 years, allozymes, microsatellites and Sanger sequence data have mainly been used
576 to investigate the population histories of Pacific shore fishes ; inferences based on
577 SNPs are still scarce (Crane et al., 2018; Maisano Delser et al., 2019). No SNP
578 mutation rate (μ) estimates were available for any of the species of this study. Yet,
579 Brumfield, Beerli, Nickerson, & Edwards, (2003) suggest that SNPs should have
580 relatively low mutation rates, of the order of 10^{-8}–10^{-9}. For fishes, a large array of
581 mutation rates have been hypothesized. To our knowledge, these range from 2.5 x 10^{-}
582 ^{8} (Kavembe, Kautt, Machado-Schiaffino, & Meyer, 2016; Nunziata & Weisrock, 2018)
583 using a SNP mutation rate calibrated on humans (Excoffier, Dupanloup, Huerta-
584 Sánchez, Sousa, & Foll, 2013b) to as slow as 3.5 x 10^{-9} (Malinsky et al., 2018) using
585 mutation rate estimated in three Lake Malawi cichlids comparing the genotypes of
586 parents and their offspring. The SNP mutation rate we chose (1 x 10^{-8}) corresponds to
587 one of the most often used in the literature for fishes (Jacobs et al., 2018; Le Moan et
588 al., 2016; Rougeux et al., 2017; Souissi et al., 2018; Tine et al., 2014) and is in
589 accordance with Brumfield, Beerli, Nickerson, & Edwards, (2003). With this mutation
590 rate, we found relatively high estimates of the effective population sizes (10^5 to 10^6);
591 yet a mutation rate of 10^{-9} would have led to even higher estimates, which is less likely

592 considering the fact that the species studied here have very restricted distributions. In
593 the same manner, our estimates of the expansion times found with this mutation rate
594 are in agreement with previous studies of the demographic history of Pacific reef fishes
595 based on mitochondrial sequence data (Delrieu-Trottin et al., 2017; Dibattista, Rocha,
596 Craig, Feldheim, & Bowen, 2012; Gaither et al., 2010), which have recovered
597 population expansions during the last 400,000 years. Generation times can also
598 strongly bias estimates, resulting for instance in synchronous population fluctuations
599 among species with similar generation times. Alternatively, applying erroneous
600 generation times to species with similar demographic trajectories can lead to the
601 spurious inference of asynchronous demographic changes. In order to use generation
602 time estimates that are as accurate as possible, we selected generation times of close
603 relatives and of similar sized species from the literature for most species (**TABLE 1**).
604 The fact that the most recent demographic change was found for the species with the
605 greatest generation time (*Cantherines rapanui,* 3 years) and the Cluster of
606 coexpanding species (Cluster 1) comprises five species with three different
607 generations times together suggest that the synchronous demographic expansions
608 inferred here are not spurious and results from community dynamics associated with
609 eustatic changes. This being said, estimates of generation times and mutation rates
610 for more species of fishes will strengthen future demographic analyses.
611

612 **5 | CONCLUSIONS**

613 We elucidate for the first time the demographic history of the Rapa Nui endemic
614 reef fish community using genomic data. We show that the Rapa Nui reef fish endemic
615 community shares a common history, with expansions occurring during the last glacial
616 period for the two different types of endemic species. Local processes based on the
617 seamount system around Rapa Nui have played a major role in the foundation and
618 persistence of this endemic reef fish community through dynamic colonization /
619 extinction / recolonization events throughout the Rapa Nui Archipelago. Altogether, our
620 results reflect the importance of working at the community level, i.e. exploring multiple
621 species to uncover general trends. Finally, our results provide insights on the
622 mechanisms by which peripheral endemism has originated in coral reef fishes.
623

ACKNOWLEDGEMENTS

We thank Rebeca Tepano, Nina, Taveke Olivares Rapu, Liza Garrido Toleado (SERNAPESCA), Ludovic Tuki (Mesa del Mar, Te Mau O Te Vaikava O Rapa Nui), and the people of the Rapa Nui Island for their kind and generous support. We thank Luiz A. Rocha for kindly sharing photographs and information related to maximum depth of several Rapa Nui endemic species. We are grateful to the Genotoul bioinformatics platform Toulouse Midi-Pyrenees (Bioinfo Genotoul; http://bioinfo.genotoul.fr/) for providing computing resources. We are obliged to three anonymous reviewers for their constructive and helpful advices. This work was supported by the FONDECYT Postdoctorado fellowship N°3160692 to E. Delrieu-Trottin and by the ATM grant 2016 from the Muséum National d'Histoire Naturelle to Stefano Mona. E.C.Giles thanks the scholarship BECA CONICYT-PCHA/Doctorado Nacional Chile/2019 Folio No. 21190878. P. Saenz-Agudelo was supported by FONDECYT grant N°1190710.

ETHICS

All applicable institutional guidelines for the care and use of animals were followed. Specimens were collected under permit No. 724, 8 March 2016 obtained from the Chilean Subsecretary of Fishing. The Universidad Austral de Chile Ethical Care Committee and Biosecurity Protocol approved our use and handling of animals.

CONFLICT OF INTEREST

None declared.

AUTHOR CONTRIBUTIONS

E.D.-T. and P.S.-A. conceived the study; E.D.-T., P.S.-A. and S.M. acquired the funding; E.D.-T., E.C.G., V.N, C.R.E. and P.S.-A., collected the field data; E.D.-T., P.C.- B. and A.S. produced the data; E.D.-T., N.H., S.M, and P.S.-A. analyzed the data; E.D.-T., N.H., E.C.G., S.M, and P.S.-A wrote the manuscript. All authors gave final approval for publication.

DATA ACCESSIBILITY

All Fastq sequence files are available from the GenBank at the National Center for Biotechnology Information short-read archive database (BioProject accession number: PRJNA622670).

ORCID

Erwan Delrieu-Trottin https://orcid.org/0000-0002-4120-9316

Nicolas Hubert https://orcid.org/0000-0001-9248-3377

Emily C. Giles https://orcid.org/0000-0002-3297-3013

Stefano Mona https://orcid.org/0000-0001-9087-0656

Pablo Saenz-Agudelo https://orcid.org/0000-0001-8197-2861

REFERENCES

Allen, G. R. (2008). Conservation hotspots of biodiversity and endemism for Indo-Pacific coral reef fishes. *Aquatic Conservation: Marine and Freshwater Ecosystems*, *18*(5), 541–556. doi:10.1002/aqc.880

Allen, G. R., & Erdmann, M. (2012). Reef fishes of the East Indies. *…I--III. Tropical Reef …*, 1292. Retrieved from http://www.uhpress.hawaii.edu/p-8881-9780987260000.aspx

Augustin, L., Barbante, C., Barnes, P. R. F., Barnola, J. M., Bigler, M., Castellano, E., … EPICA community members. (2004). Eight glacial cycles from an Antarctic ice core. *Nature*. doi:10.1038/nature02599

Avise, J. C. (2009). Phylogeography: retrospect and prospect. *Journal of Biogeography*, *36*(1), 3–15.

Bard, E., Hamelin, B., Arnold, M., Montaggioni, L., Cabioch, G., Faure, G., & Rougerie, F. (1996). Deglacial sea-level record from Tahiti corals and the timing of global meltwater discharge. *Nature*, *382*(6588), 241–244. doi:10.1038/382241a0

Beaumont, M. A., Zhang, W., & Balding, D. J. (2002). Approximate Bayesian computation in population genetics. *Genetics*.

Bellwood, D. R., & Wainwright, P. C. (2002). The History and Biogeography of Fishes on Coral Reefs. In *Coral Reef Fishes* (pp. 5–32). doi:10.1016/B978-012615185-5/50003-7

Bowen, B. W., Muss, A., Rocha, L. A., & Grant, W. S. (2006). Shallow mtDNA coalescence in Atlantic pygmy angelfishes (genus Centropyge) indicates a recent invasion from the Indian Ocean. *Journal of Heredity*, *97*(1), 1–12. doi:10.1093/jhered/esj006

Breiman, L., Friedman, J. H., Olshen, R. A., & Stone, C. J. (1984). Classification and regression trees. Belmont, CA: Wadsworth. *International Group*, *432*, 151–166.

Brumfield, R. T., Beerli, P., Nickerson, D. A., & Edwards, S. V. (2003). The utility of single nucleotide polymorphisms in inferences of population history. *Trends in Ecology and Evolution*, *18*(5), 249–256. doi:10.1016/S0169-5347(03)00018-1

Burbrink, F. T., Chan, Y. L., Myers, E. A., Ruane, S., Smith, B. T., & Hickerson, M. J. (2016). Asynchronous demographic responses to Pleistocene climate change in Eastern Nearctic vertebrates. *Ecology Letters*, *19*(12), 1457–1467. doi:10.1111/ele.12695

Catchen, J., Hohenlohe, P. A., Bassham, S., Amores, A., & Cresko, W. A. (2013). Stacks: An analysis tool set for population genomics. *Molecular Ecology*, *22*(11), 3124–3140. doi:10.1111/mec.12354

Catchen, J. M., Amores, A., Hohenlohe, P., Cresko, W., & Postlethwait, J. H. (2011). Stacks : Building and Genotyping Loci De Novo From Short-Read Sequences. *G3 Genes|Genomes|Genetics*, *1*(3), 171–182. doi:10.1534/g3.111.000240

Cea, A. (2016). *Ika Rapa Nui*. Rapa Nui Press.

Chan, Y. L., Schanzenbach, D., & Hickerson, M. J. (2014). Detecting concerted demographic response across community assemblages using hierarchical approximate Bayesian computation. *Molecular Biology and Evolution*, *31*(9), 2501–2515. doi:10.1093/molbev/msu187

Clark, P. U., Dyke, A. S., Shakun, J. D., Carlson, A. E., Clark, J., Wohlfarth, B., … McCabe, A. M. (2009). The last glacial maximum. *Science*, *325*(5941), 710–714.

Clouard, V., & Bonneville, A. (2005). Ages of seamounts, islands, and plateaus on the Pacific plate. *Special Paper 388: Plates, Plumes and Paradigms*, *388*, 71–90. doi:10.1130/0-8137-2388-4.71

Craig, M. T., Eble, J. A., & Bowen, B. W. (2010). Origins, ages and population histories: Comparative phylogeography of endemic Hawaiian butterflyfishes (genus Chaetodon). *Journal of Biogeography*, *37*(11), 2125–2136. doi:10.1111/j.1365-2699.2010.02358.x

Craig, M. T., Eble, J. A., Bowen, B. W., & Robertson, D. R. (2007a). High genetic connectivity across the Indian and Pacific Oceans in the reef fish Myripristis berndti (Holocentridae). *Marine Ecology Progress Series*, *334*, 245–254. doi:10.3354/meps334245

Craig, M. T., Eble, J. A., Bowen, B. W., & Robertson, D. R. (2007b). High genetic connectivity across the Indian and Pacific Oceans in the reef fish Myripristis berndti (Holocentridae). *Marine Ecology Progress Series*, *334*, 245–254. doi:10.3354/meps334245

Crandall, E. D., Frey, M. A., Grosberg, R. K., & Barber, P. H. (2008). Contrasting demographic history and phylogeographical patterns in two Indo-Pacific gastropods. *Molecular Ecology*, *17*(2), 611–626. doi:10.1111/j.1365-294X.2007.03600.x

Crane, N. L., Tariel, J., Caselle, J. E., Friedlander, A. M., Ross Robertson, D., & Bernardi, G. (2018). Clipperton Atoll as a model to study small marine populations: Endemism and the genomic consequences of small population size. *PLoS ONE*. doi:10.1371/journal.pone.0198901

Cutler, K. B., Edwards, R. L., Taylor, F. W., Cheng, H., Adkins, J., Gallup, C. D., … Bloom, A. L. (2003). Rapid sea-level fall and deep-ocean temperature change since the last interglacial period. *Earth and Planetary Science Letters*, *206*(3–4), 253–271.

De'ath, G. (2002). Multivariate Regression Tree: A New Technique for Modeling Species–Environment Relationships. *Ecology*, *83*(4), 1105–1117. doi:10.1890/0012-9658(2002)083[1105:MRTANT]2.0.CO;2

Delrieu-Trottin, E., Brosseau-Acquaviva, L., Mona, S., Neglia, V., Giles, E. C., Rapu-

Edmunds, C., & Saenz-Agudelo, P. (2019). Understanding the origin of the most isolated endemic reef fish fauna of the Indo-Pacific: Coral reef fishes of Rapa Nui. *Journal of Biogeography*, *46*(January), 723–733. doi:10.1111/jbi.13531

Delrieu-Trottin, E., Maynard, J., & Planes, S. (2014). Endemic and widespread coral reef fishes have similar mitochondrial genetic diversity. *Proceedings of the Royal Society B: Biological Sciences*, *281*(1797). doi:10.1098/rspb.2014.1068

Delrieu-Trottin, E., Mona, S., Maynard, J., Neglia, V., Veuille, M., & Planes, S. (2017). Population expansions dominate demographic histories of endemic and widespread Pacific reef fishes. *Scientific Reports*, *7*(January), 40519. doi:10.1038/srep40519

Delrieu-Trottin, E., Williams, J. T., Bacchet, P., Kulbicki, M., Mourier, J., Galzin, R., … Planes, S. (2015). Shore fishes of the Marquesas Islands, an updated checklist with new records and new percentage of endemic species. *Check List*, *11*(5). doi:10.15560/11.5.1758

Dibattista, J. D., Rocha, L. A., Craig, M. T., Feldheim, K. A., & Bowen, B. W. (2012). Phylogeography of two closely related indo-pacific butterflyfishes reveals divergent evolutionary histories and discordant results from mtDNA and microsatellites. *Journal of Heredity*, *103*(5), 617–629. doi:10.1093/jhered/ess056

Drummond, A J, Rambaut, A., Shapiro, B., & Pybus, O. G. (2005). Bayesian coalescent inference of past population dynamics from molecular sequences. *Molecular Biology and Evolution*, *22*(5), 1185–1192. doi:10.1093/molbev/msi103

Drummond, Alexei J, & Rambaut, A. (2007). BEAST: Bayesian evolutionary analysis by sampling trees. *BMC Evolutionary Biology*, *7*(1), 214. doi:10.1186/1471-2148-7-214

Easton, E. E., Sellanes, J., Berkenpas, E., Gaymer, C. F., Morales, N., & Gorny, M. (2017). Diversity of deep-sea fi shes of the Easter Island Ecoregion. *Deep-Sea Research Part II*, *137*(December 2016), 78–88. doi:10.1016/j.dsr2.2016.12.006

Eschmeyer, W. N., Fricke, R., Fong, J. D., & Polack, D. A. (2010). Marine fish diversity: History of knowledge and discovery (Pisces). *Zootaxa*, *2525*(2525), 19–50. Retrieved from www.mapress.com/zootaxa/

Excoffier, L., Dupanloup, I., Huerta-Sánchez, E., Sousa, V. C., & Foll, M. (2013a). Robust Demographic Inference from Genomic and SNP Data. *PLoS Genetics*, *9*(10). doi:10.1371/journal.pgen.1003905

Excoffier, L., Dupanloup, I., Huerta-Sánchez, E., Sousa, V. C., & Foll, M. (2013b). Robust Demographic Inference from Genomic and SNP Data. *PLoS Genetics*. doi:10.1371/journal.pgen.1003905

Fauvelot, C., Bernardi, G., & Planes, S. (2003). Reductions in the mitochondrial DNA diversity of coral reef fish provide evidence of population bottlenecks resulting from Holocene sea-level change. *Evolution; International Journal of Organic Evolution*, *57*(7), 1571–1583. doi:10.1111/j.0014-3820.2003.tb00365.x

Friedlander, A. M., Ballesteros, E., Beets, J., Berkenpas, E., Gaymer, C. F., Gorny, M., & Sala, E. (2013). Effects of isolation and fishing on the marine ecosystems of Easter Island and Salas y Gómez, Chile. *Aquatic Conservation: Marine and Freshwater Ecosystems*, *23*(4), 515–531. doi:10.1002/aqc.2333

Froese, R., & Binohlan, C. (2000). Empirical relationships to estimate asymptotic length, length at first maturity and length at maximum yield per recruit in fishes, with a simple method to evaluate length frequency data. *Journal of Fish Biology*, *56*(4), 758–773. doi:10.1111/j.1095-8649.2000.tb00870.x

Gaboriau, T., Leprieur, F., Mouillot, D., & Hubert, N. (2018). Influence of the geography of speciation on current patterns of coral reef fish biodiversity across the Indo-Pacific. *Ecography*, *41*(8), 1295–1306. doi:10.1111/ecog.02589

Gaither, M. R., Toonen, R. J., Robertson, D. R., Planes, S., & Bowen, B. W. (2010). Genetic evaluation of marine biogeographical barriers: Perspectives from two widespread Indo-Pacific snappers (Lutjanus kasmira and Lutjanus fulvus). *Journal of Biogeography*, *37*(1), 133–147. doi:10.1111/j.1365-2699.2009.02188.x

Gajdzik, L., Bernardi, G., Lepoint, G., & Frédérich, B. (2018). Genetic diversity mirrors trophic ecology in coral reef fish feeding guilds. *Molecular Ecology*, *27*(24), 5004–5018. doi:10.1111/mec.14936

Heled, J., & Drummond, A. J. (2008). Bayesian inference of population size history from multiple loci. *BMC Evolutionary Biology*, *8*(1), 289. doi:10.1186/1471-2148-8-289

Hellberg, M. E. (2001). Climate-Driven Range Expansion and Morphological Evolution in a Marine Gastropod. *Science*, *292*(5522), 1707–1710. doi:10.1126/science.1060102

Hewitt, G. (2003). Ice ages: their impact on species distributions and evolution. In *Evolution on Planet Earth (eds. L.J. Rothschild & A.M Lister)* (pp. 339–361). Academic Press.

Hewitt, G. M. (2001). Speciation, hybrid zones and phylogeography--or seeing genes in space and time. *Molecular Ecology*, *10*(3), 537–549. doi:doi:10.1046/j.1365-294x.2001.01202.x

Hewitt, G. M. (2004). The structure of biodiversity – insights from molecular phylogeography. *Frontiers in Zoology*, *1*(1), 4. doi:10.1186/1742-9994-1-4

Hickerson, M. J., Carstens, B. C., Cavender-Bares, J., Crandall, K. A., Graham, C. H., Johnson, J. B., … Yoder, A. D. (2010). Phylogeography's past, present, and future: 10 years after. *Molecular Phylogenetics and Evolution*, *54*(1), 291–301.

Horne, J. B., van Herwerden, L., Choat, J. H., & Robertson, D. R. (2008). High population connectivity across the Indo-Pacific: Congruent lack of phylogeographic structure in three reef fish congeners. *Molecular Phylogenetics and Evolution*, *49*(2), 629–638. doi:10.1016/j.ympev.2008.08.023

Hughes, T. P., Bellwood, D. R., & Connolly, S. R. (2002). Biodiversity hotspots, centres of endemicity, and the conservation of coral reefs. *Ecology Letters*, *5*(6), 775–784. doi:10.1046/j.1461-0248.2002.00383.x

Jacobs, A., Hughes, M., Robinson, P., Adams, C., & Elmer, K. (2018). The Genetic Architecture Underlying the Evolution of a Rare Piscivorous Life History Form in Brown Trout after Secondary Contact and Strong Introgression. *Genes*, *9*(6), 280. doi:10.3390/genes9060280

Jombart, T. (2008). Adegenet: A R package for the multivariate analysis of genetic markers. *Bioinformatics*, *24*(11), 1403–1405. doi:10.1093/bioinformatics/btn129

Jombart, T., & Ahmed, I. (2011). adegenet 1.3-1: New tools for the analysis of genome-wide SNP data. *Bioinformatics*, *27*(21), 3070–3071. doi:10.1093/bioinformatics/btr521

Jump, A. S., & Penuelas, J. (2005). Running to stand still: adaptation and the response of plants to rapid climate change. *Ecology Letters*, *8*(9), 1010–1020.

Kavembe, G. D., Kautt, A. F., Machado-Schiaffino, G., & Meyer, A. (2016). Eco-morphological differentiation in Lake Magadi tilapia, an extremophile cichlid fish

living in hot, alkaline and hypersaline lakes in East Africa. *Molecular Ecology*, *25*(7), 1610–1625. doi:10.1111/mec.13461

Klanten, O. S., Choat, J. H., & Van Herwerden, L. (2007). Extreme genetic diversity and temporal rather than spatial partitioning in a widely distributed coral reef fish. *Marine Biology*, *150*(4), 659–670. doi:10.1007/s00227-006-0372-7

Knaus, B. J., & Grünwald, N. J. (2017). vcfr: a package to manipulate and visualize variant call format data in R. *Molecular Ecology Resources*, *17*(1), 44–53. doi:10.1111/1755-0998.12549

Lapierre, M., Lambert, A., & Achaz, G. (2017). Accuracy of Demographic Inferences from the Site Frequency Spectrum : The Case of the, *206*(May), 439–449. doi:10.1534/genetics.116.192708/-/DC1.1

Le Moan, A., Gagnaire, P. A., & Bonhomme, F. (2016). Parallel genetic divergence among coastal-marine ecotype pairs of European anchovy explained by differential introgression after secondary contact. *Molecular Ecology*. doi:10.1111/mec.13627

Lessa, E. P., Cook, J. A., & Patton, J. L. (2003). Genetic footprints of demographic expansion in North America, but not Amazonia, during the Late Quaternary. *Proceedings of the National Academy of Sciences*, *100*(18), 10331–10334.

Liu, X., & Fu, Y. X. (2015). Exploring population size changes using SNP frequency spectra. *Nature Genetics*, *47*(5), 555–559. doi:10.1038/ng.3254

Ludt, W. B., & Rocha, L. A. (2015). Shifting seas: The impacts of Pleistocene sea-level fluctuations on the evolution of tropical marine taxa. *Journal of Biogeography*, *42*(1), 25–38. doi:10.1111/jbi.12416

Maisano Delser, P., Corrigan, S., Duckett, D., Suwalski, A., Veuille, M., Planes, S., … Mona, S. (2019). Demographic inferences after a range expansion can be biased: the test case of the blacktip reef shark (Carcharhinus melanopterus). *Heredity*. doi:10.1038/s41437-018-0164-0

Maisano Delser, P., Corrigan, S., Hale, M., Li, C., Veuille, M., Planes, S., … Mona, S. (2016). Population genomics of C. melanopterus using target gene capture data: demographic inferences and conservation perspectives. *Scientific Reports*, *6*(1), 33753. doi:10.1038/srep33753

Malinsky, M., Svardal, H., Tyers, A. M., Miska, E. A., Genner, M. J., Turner, G. F., & Durbin, R. (2018). Whole-genome sequences of Malawi cichlids reveal multiple radiations interconnected by gene flow. *Nature Ecology and Evolution*, *2*(12), 1940–1955. doi:10.1038/s41559-018-0717-x

Mastretta-Yanes, A., Arrigo, N., Alvarez, N., Jorgensen, T. H., Piñero, D., & Emerson, B. C. (2015). Restriction site-associated DNA sequencing, genotyping error estimation and de novo assembly optimization for population genetic inference. *Molecular Ecology Resources*, *15*(1), 28–41. doi:10.1111/1755-0998.12291

McManus, J. F. (2004). A great grand-daddy of ice cores. *Nature*. doi:10.1038/429611a

Miller, K. G., Miller, K. G., Kominz, M. A., Browning, J. V, Wright, J. D., Mountain, G. S., … Pekar, S. F. (2005). The Phanerozoic Record of Global Sea-Level Change. *Science*, *310*, 1293–1298. doi:10.1126/science.1116412

Newman, W., & Foster, B. (1983). The Rapanuian faunal district (Easter and Sala y Gomez): in search of ancient archipelagos. *Bulletin of Marine Science*, *33*(3), 633–644.

Nunziata, S. O., & Weisrock, D. W. (2018). Estimation of contemporary effective

population size and population declines using RAD sequence data. *Heredity*, *120*(3), 196–207. doi:10.1038/s41437-017-0037-y

Oksanen, J., Blanchet, F. G., Kindt, R., Legendre, P., Minchin, P. R., O'Hara, R. B., … Wagner, H. (2012). vegan: Community Ecology Package. R package version 2.1-20/r2309. *Www.R-Project.Org.*, 1–255. Retrieved from http://r-forge.r-project.org/projects/vegan/

Pahnke, K., Zahn, R., Elderfield, H., & Schulz, M. (2003). 340,000-year centennial-scale marine record of Southern Hemisphere climatic oscillation. *Science*, *301*(5635), 948–952.

Pante, E., & Simon-Bouhet, B. (2013). marmap: A Package for Importing, Plotting and Analyzing Bathymetric and Topographic Data in R. *PLOS ONE*, *8*(9), 1–4. doi:10.1371/journal.pone.0073051

Paradis, E. (2010). pegas: an {R} package for population genetics with an integrated--modular approach. *Bioinformatics*, *26*, 419–420.

Peterson, B. K., Weber, J. N., Kay, E. H., Fisher, H. S., & Hoekstra, H. E. (2012). Double digest RADseq: An inexpensive method for de novo SNP discovery and genotyping in model and non-model species. *PLoS ONE*, *7*(5). doi:10.1371/journal.pone.0037135

Petit, R. J., Aguinagalde, I., de Beaulieu, J.-L., Bittkau, C., Brewer, S., Cheddadi, R., … others. (2003). Glacial refugia: hotspots but not melting pots of genetic diversity. *Science*, *300*(5625), 1563–1565.

Pfeifer, B., Wittelsbürger, U., Ramos-Onsins, S. E., & Lercher, M. J. (2014). PopGenome: An efficient swiss army knife for population genomic analyses in R. *Molecular Biology and Evolution*, *31*(7), 1929–1936. doi:10.1093/molbev/msu136

Pinheiro, H. T., Bernardi, G., Simon, T., Joyeux, J.-C., Macieira, R. M., Gasparini, J. L., … Rocha, L. A. (2017). Island biogeography of marine organisms. *Nature*, *549*, 82. Retrieved from http://dx.doi.org/10.1038/nature23680

Pybus, O. G., Rambaut, A., & Harvey, P. H. (2000). An integrated framework for the inference of viral population history from reconstructed genealogies. *Genetics*, *155*(3), 1429–1437. doi:10.1073/pnas.88.5.1597

R Core Team. (2017). R: A Language and Environment for Statistical Computing. *R Foundation for Statistical Computing, Vienna, Austria*. doi:http://www.R-project.org/

Randall, J. E. (1998). Review Article Zoogeography of Shore Fishes of the Indo-Pacific Region. *ZOOLOGICAL STUDIES*, *37*, 227–268. Retrieved from http://www.sinica.edu.tw/zool/zoolstud/Journals/37.4/227.pdf

Randall, J. E. (2005). *Reef and Shore Fishes of the South Pacific : New Caledonia to Tahiti and the Pitcairn Islands* (Vol. 1). University of Hawai'i Press Honolulu.

Randall, J. E. (2007). *Reef fishes of Hawaii*. University of Hawai'i Press Honolulu.

Randall, J. E., & Cea, A. (2011). *Shore Fishes of Easter Island*. University of Hawai'i Press. Retrieved from http://books.google.com/books?hl=en&lr=&id=iXtCTSRTcb8C&pgis=1

Ray, J. S., Mahoney, J. J., Duncan, R. A., Ray, J., Wessel, P., & Naar, D. F. (2012). Chronology and geochemistry of lavas from the Nazca Ridge and Easter Seamount Chain: An ~30 myr hotspot record. *Journal of Petrology*, *53*(7), 1417–1448. doi:10.1093/petrology/egs021

Reid, B. N., Naro-Maciel, E., Hahn, A. T., FitzSimmons, N. N., & Gehara, M. (2019).

Geography best explains global patterns of genetic diversity and postglacial co-expansion in marine turtles. *Molecular Ecology*, *28*(14), 3358–3370. doi:10.1111/mec.15165

Robertson, D. R. (2004). High genetic diversities and complex genetic structure in an Indo-Paci c tropical reef sh (Chlorurus sordidus): evidence of an unstable evolutionary past? *Marine Biology*, 757–767. doi:10.1007/s00227-003-1224-3

Rocha, L. A., Pinheiro, H. T., Shepherd, B., Papastamatiou, Y. P., Luiz, O. J., Pyle, R. L., & Bongaerts, P. (2018). Mesophotic coral ecosystems are threatened and ecologically distinct from shallow water reefs. *Science*, *361*(6399), 281–284. doi:10.1126/science.aaq1614

Rougeux, C., Bernatchez, L., & Gagnaire, P. A. (2017). Modeling the multiple facets of speciation-with-gene-flow toward inferring the divergence history of lake whitefish species pairs (Coregonus clupeaformis). *Genome Biology and Evolution*, *9*(8), 2057–2074. doi:10.1093/gbe/evx150

Souissi, A., Bonhomme, F., Manchado, M., Bahri-Sfar, L., & Gagnaire, P. A. (2018). Genomic and geographic footprints of differential introgression between two divergent fish species (Solea spp.). *Heredity*. doi:10.1038/s41437-018-0079-9

Therneau, T. M., Oksanen, B. R., Oksanen, J., Atkinson, B., & De'ath, G. (2014). mvpart: Multivariate partitioning. Retrieved from https://cran.r-project.org/package=mvpart

Tine, M., Kuhl, H., Gagnaire, P.-A., Louro, B., Desmarais, E., Martins, R. S. T., … Reinhardt, R. (2014). European sea bass genome and its variation provide insights into adaptation to euryhalinity and speciation. *Nature Communications*, *5*(May), 5770. doi:10.1038/ncomms6770

Vrba, E. S. (1992). Mammals as a key to evolutionary theory. *Journal of Mammalogy*, *73*(1), 1–28.

Wakeley, J. (2009). *Coalescent theory: an introduction*. (ed. Greenwood Village, Colorado: Roberts & Company Publishers)

Wakeley, J. (2010). Natural Selection and Coalescent Theory. *Evolution since Darwin: The First 150 Years*, 119–149. doi:10.1016/B978-012323448-3/50010-6

Wickham, H. (2009). *ggplot2: Elegant Graphics for Data Analysis*. Springer-Verlag New York. Retrieved from http://ggplot2.org

Winters, K. L., van Herwerden, L., Choat, J. H., & Robertson, D. R. (2010). Phylogeography of the Indo-Pacific parrotfish Scarus psittacus: Isolation generates distinctive peripheral populations in two oceans. *Marine Biology*, *157*(8), 1679–1691. doi:10.1007/s00227-010-1442-4

Wong, B., & Candolin, U. (2015). Behavioral responses to changing environments. *Behavioral Ecology*, *26*(3), 665–673.

Woodroffe, C. D., Brooke, B. P., Linklater, M., Kennedy, D. M., Jones, B. G., Buchanan, C., … Zhao, J. X. (2010). Response of coral reefs to climate change: Expansion and demise of the southernmost pacific coral reef. *Geophysical Research Letters*, *37*(15), L15602. doi:10.1029/2010GL044067

Xue, A. T., & Hickerson, M. J. (2015). The aggregate site frequency spectrum for comparative population genomic inference. *Molecular Ecology*, *24*(24), 6223–6240. doi:10.1111/mec.13447

985 **Figure captions**

986 **FIGURE 1 (A)** Multivariate regression tree (MRT) of normalized summary statistics
987 using as predictor variables range-size classification (large-range endemic and small-
988 range endemic), demographic pattern (expansion, bottleneck), reproductive strategy
989 (pelagic eggs, demersal eggs and mouth brooding), and generation time; **(B)**
990 Aggregated SFS for the nine species being studied. Colors denote the clusters
991 retrieved by the MRT analysis.

992

993 **FIGURE 2** ABC skyline plots representing the variation of the median effective
994 population size through time and sea level fluctuations for the past 400,000 years using
995 data from (Miller et al., 2005). Dark tones indicate inter-glacial periods characterized
996 by sea level rises while grey tones indicate glacial periods with lower sea levels.

997

998 **FIGURE 3** *Stairwayplots* (black) (red) and abc skylines (pink) representing variation in
999 effective population size through time and sea level fluctuations for the past 400,000
1000 years using data from (Miller et al., 2005). Only median Ne is represented for the abc
1001 skyline plots while median and 97.5% interval values are represented for the
1002 *stairwayplots*. Dark tones indicate inter-glacial periods characterized by sea level rises
1003 while grey tones indicate glacial periods with lower sea level.

1004

1005 **FIGURE 4** Posterior estimates for the different parameters of the hABC analysis: (A)
1006 the frequency of coexpansion (ζ) , (B) the co−expansion time (τ), and (C) the total
1007 mean expansion time E (τ).

1008

1009 **FIGURE 5** Surface of potential habitat for Rapa Nui endemic reef fish species
1010 represented for present conditions (red) and during sea level lowstand conditions with
1011 sea level as low as -120m compared to present sea level (orange).

1012

1013 **Supplementary Material.**

FIGURE S1 Multivariate regression tree (MRT) of normalized summary statistics using as predictor variables range-size classification (large-range endemic and small-range endemic), demographic pattern (expansion, bottleneck), reproductive strategy (pelagic eggs, demersal eggs and mouth brooding), and generation time.

FIGURE S2 Cross-validation for ζ after 1,000 simulations from prior distributions. X-axe: simulated ζ. Y-axe: estimated ζ through the same ABC procedure implemented for the real data.

FIGURE S3 PCA computed on the posterior predictive distribution of the aSFS after 50,000 simulations. Black dot: pseudo-observed (simulated) datasets; red dot: observed data. The first two axes displayed here represent 62.98 % of the total variance.

1028 **TABLE 1** Ecological data on the species of interest of this study. Range size (S: small-range size; L: large-range size), family,
1029 reproductive strategy (p: pelagic eggs; b: demersal eggs; m: mouth brooding), maximum depth where the species have been observed
1030 (Max. depth) (1 to 5); generation time used for this study (6 to 9); maximum size of the species (Max. size) and references associated
1031 ([1]: specimens observed freediving by Cristian Rapu-Edmunds; [2]: Randall & Cea, 2011; [3]: specimens video-recorded at those depths
1032 (pers. comm. Erin Easton); [4]: Easton et al., 2017 [5]: specimens photographed at those depths by com. pers Luiz A. Rocha in 2016; [6]:
1033 Craig, Eble, Bowen, & Robertson, 2007, [7]: Bowen, Muss, Rocha, & Grant, 2006, [8]: Craig et al., 2010, [9]: Gajdzik, Bernardi, Lepoint, &
1034 Frédérich, 2018).
1035

Range size	Family	Reproductive strategy	Species	Max. depth (m)	Generation time (years)	Max. size (TL, cm)
L	Holocentridae	pelagic eggs	*Myripristis tiki*	80[1]	3[6]	26.5[2]
L	Pomacanthidae	pelagic eggs	*Centropyge hotumatua*	50[2]	1[7]	9[2]
S	Apogonidae	mouthbrooding	*Ostorhinchus chalcius*	25[2]	2	16[2]
S	Chaetodontidae	pelagic eggs	*Chaetodon litus*	156[3]	2[8]	15.5[2]
S	Holocentridae	pelagic eggs	*Sargocentron wilhlmi*	157[4]	3[6]	19.5[2]
S	Labridae	pelagic eggs	*Coris debueni*	70[2]	3	27[2]
S	Monacanthidae	benthic eggs	*Cantherhines rapanui*	20[2]	3	20[2]
S	Pomacentridae	benthic eggs	*Chrysiptera rapanui*	75[2,3]	1[9]	7.8[2]
S	Pomacentridae	benthic eggs	*Chromis randalli*	105[5]	2[9]	15[2]

1036
1037

1038 **TABLE 2** Summary of genetic data for each species. Sample size (*N*) and molecular metrics for each species of the study. Observed
1039 (Ho) and expected (He) heterozygosity computed on all sites of variable loci; Watterson's theta (Θ_w) computed on all sites of variable
1040 loci, mean pairwise differences (π) computed on all sites of variable loci, and inbreeding coefficient (FIS), Tajima's D and Fu & Li's
1041 D. All Tajima's D are significant. Maximum (in bold) and minimum (in italics and underlined) values are highlighted for all columns.

Species	*N*	No. RAD Seq loci	No. variable RADSeq loci (%)	No. SNP (%)	Ho	He	FIS	Θ_w *(x10-4)*	π (x10-4)	Tajima's D	Fu & Li's D
Myripristis tiki	18	45,432	**28,855** (64)	**46,718 (0.85)**	0.159 (±0.021)	0.160 (±0.022)	0.025	32.54	22.23	-1.211	-1.586
Centropyge hotumatua	15	29,195	21,684 (74)	38,816 (1.09)	0.156 (±0.018)	0.158 (±0.016)	0.032	**37.65**	24.38	-1.383	-1.591
Ostorhinchus chalcius	19	**63,590**	24,019 (*38*)	32,224 (*0.42*)	0.165 (±0.024)	0.162 (±0.021)	*0.008*	*26.61*	*18.55*	-1.149	-1.726
Chaetodon litus	15	41,439	21,905 (53)	33,422 (0.67)	0.220 (±0.029)	0.219 (±0.023)	0.022	32.09	28.86	-0.395	-0.500
Sargocentron wilhelmi	16	41,234	24,207 (59)	37,861 (0.76)	0.217 (±0.028)	0.217 (±0.022)	0.026	32.36	29.19	-0.381	-0.220
Coris debueni	14	47,949	28,594 (60)	45,870 (0.79)	0.208 (±0.027)	0.209 (±0.022)	0.029	34.35	28.94	-0.624	-0.747
Cantherhines rapanui	15	44,233	20,052 (45)	*28,239* (0.53)	**0.262 (±0.032)**	**0.261 (±0.024)**	0.023	29.62	**31.63**	0.266	0.293
Chrysiptera rapanui	18	*25,331*	*19,246* **(76)**	35,735 (**1.15**)	*0.137 (±0.018)*	*0.141 (±0.017)*	0.039	37.31	22.48	-1.519	-2.277
Chromis randalli	13	34,893	24,673 (71)	43,845 (1.03)	0.161(±0.019)	0.165 (±0.017)	**0.043**	38.81	25.47	-1.378	-1.814

1042

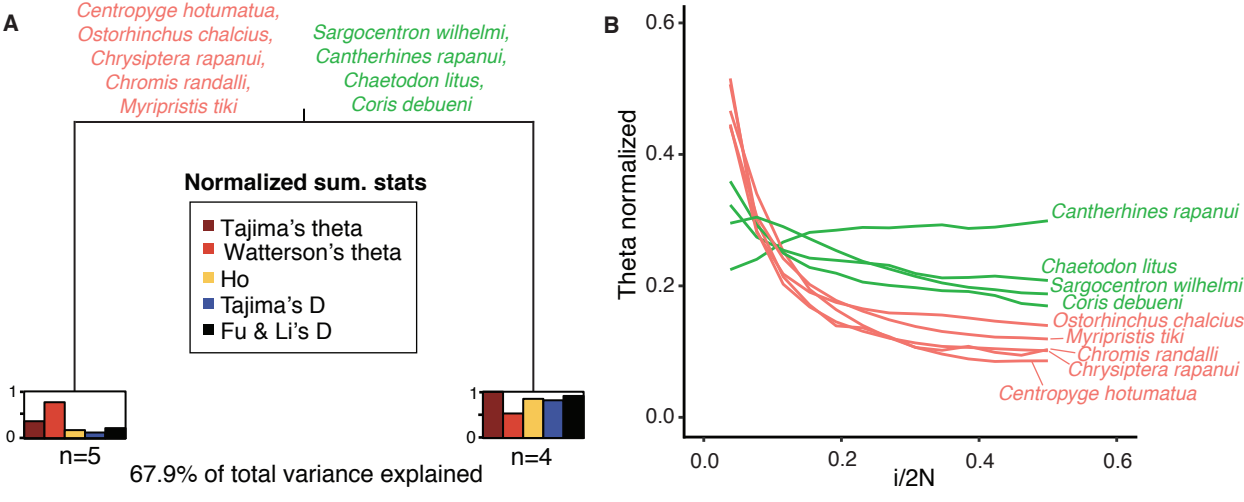
A
Centropyge hotumatua,
Ostorhinchus chalcius,
Chrysiptera rapanui,
Chromis randalli,
Myripristis tiki
Sargocentron wilhelmi,
Cantherhines rapanui,
Chaetodon litus,
Coris debueni
Normalized sum. stats
Tajima's theta
Watterson's theta
Ho
Tajima's D
Fu & Li's D
1
0
n=5
1
0
n=4
67.9% of total variance explained
B
Theta normalized
0.6
0.4
0.2
0.0
0.0
0.2
0.4
0.6
i/2N
Cantherhines rapanui
Chaetodon litus
Sargocentron wilhelmi
Coris debueni
Ostorhinchus chalcius
Myripristis tiki
Chromis randalli
Chrysiptera rapanui
Centropyge hotumatua

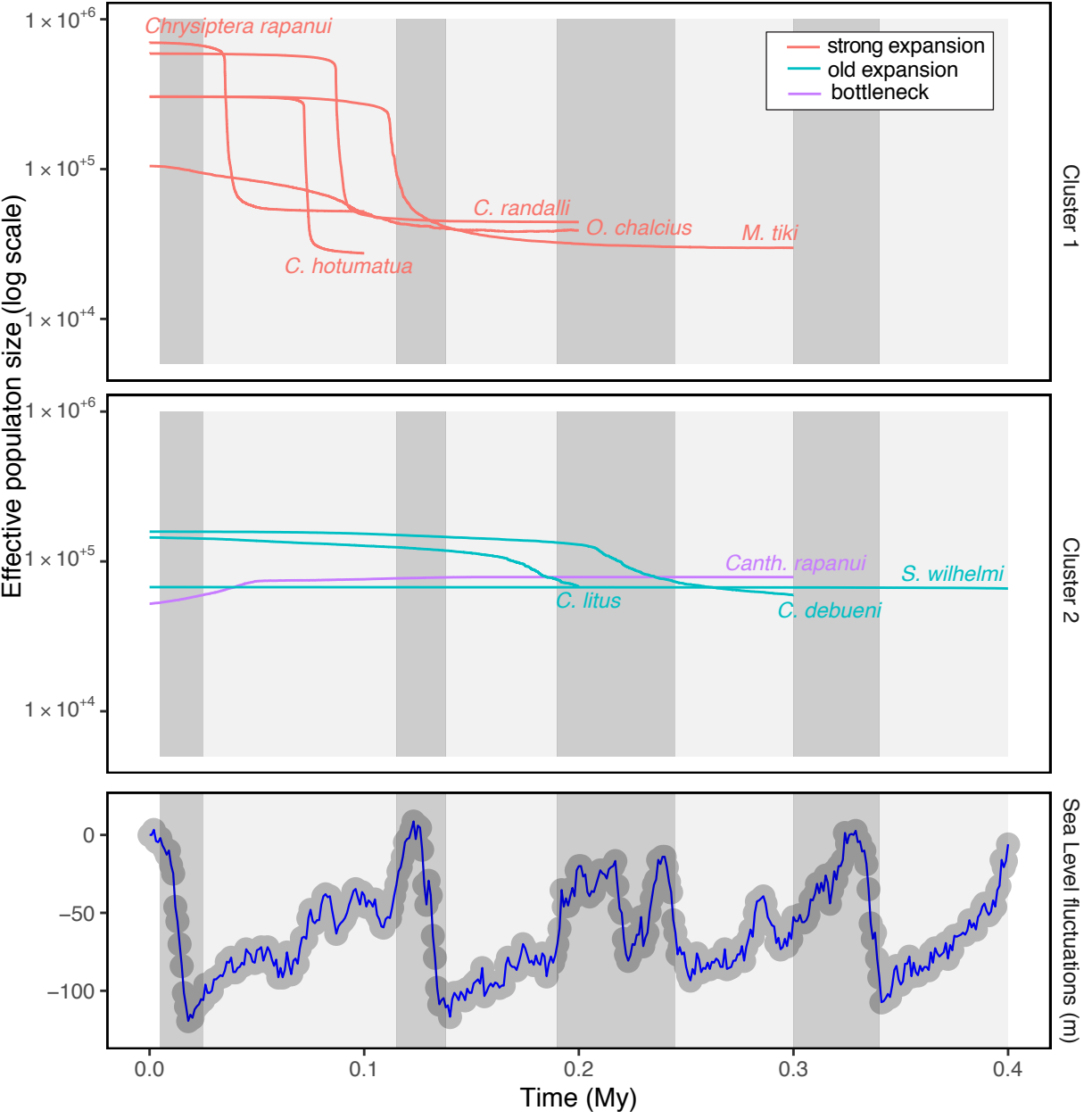
Effective populaton size (log scale)
1 × 10+6
1 × 10+5
1 × 10+4
Chrysiptera rapanui
strong expansion
old expansion
bottleneck
C. randalli
O. chalcius
M. tiki
C. hotumatua
Cluster 1
Canth. rapanui
S. wilhelmi
C. litus
C. debueni
Cluster 2
0
−50
−100
Sea Level fluctuations (m)
0.0
0.1
0.2
0.3
0.4
Time (My)

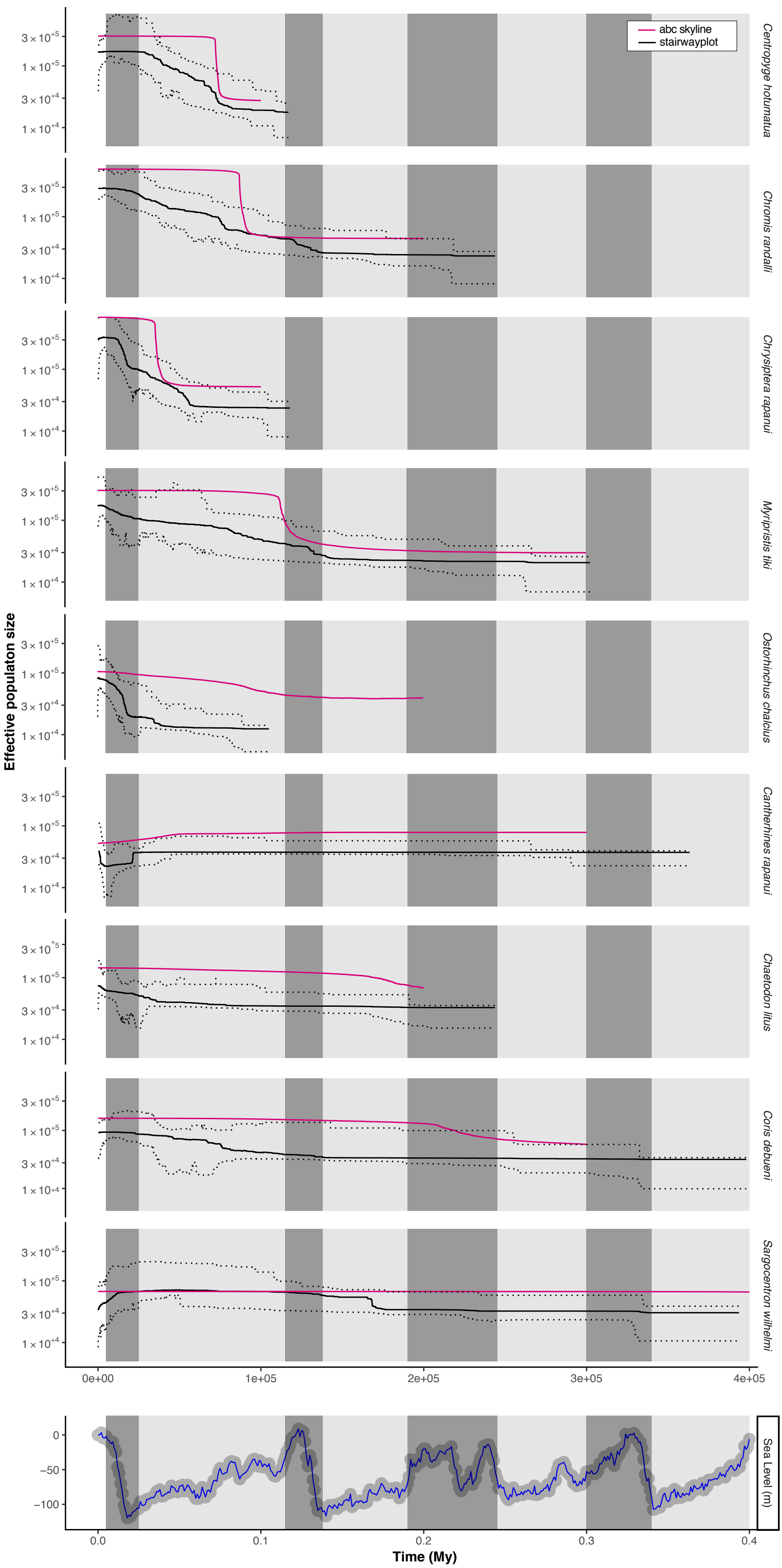
abc skyline
stairwayplot
Centropyge hotumatua
Chromis randalli
Chrysiptera rapanui
Myripristis tiki
Ostorhinchus chalcius
Cantherhines rapanui
Chaetodon litus
Coris debueni
Sargocentron wilhelmi
Effective populaton size
3 × 10+5
1 × 10+5
3 × 10+4
1 × 10+4
0e+00
1e+05
2e+05
3e+05
4e+05
Sea Level (m)
0
−50
−100
0.0
0.1
0.2
0.3
0.4
Time (My)

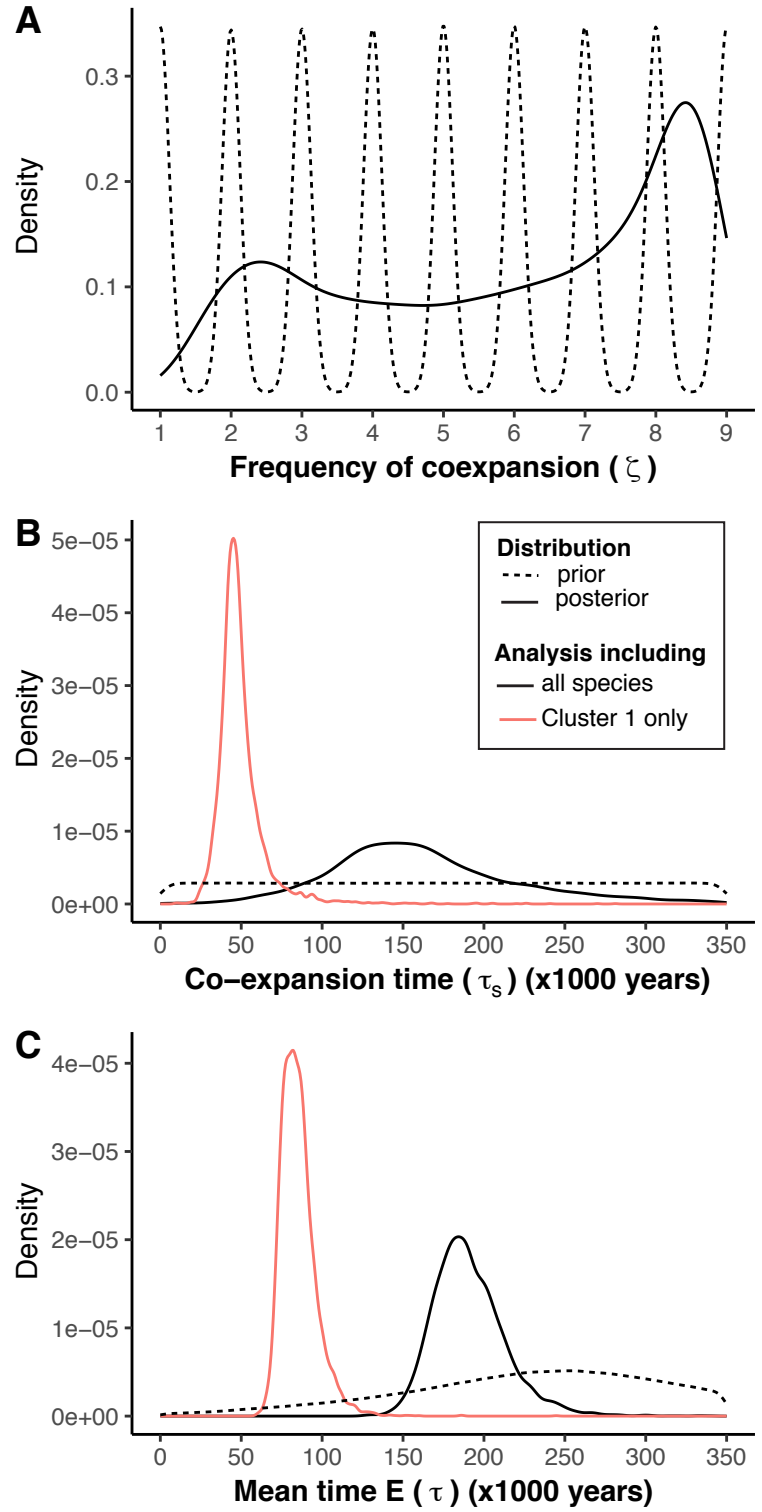
A
Density
0.0
0.1
0.2
0.3
1
2
3
4
5
6
7
8
9
Frequency of coexpansion (ζ)
B
Density
0e+00
1e−05
2e−05
3e−05
4e−05
5e−05
0
50
100
150
200
250
300
350
Co−expansion time (τs) (x1000 years)
Distribution
prior
posterior
Analysis including
all species
Cluster 1 only
C
Density
0e+00
1e−05
2e−05
3e−05
4e−05
0
50
100
150
200
250
300
350
Mean time E (τ) (x1000 years)

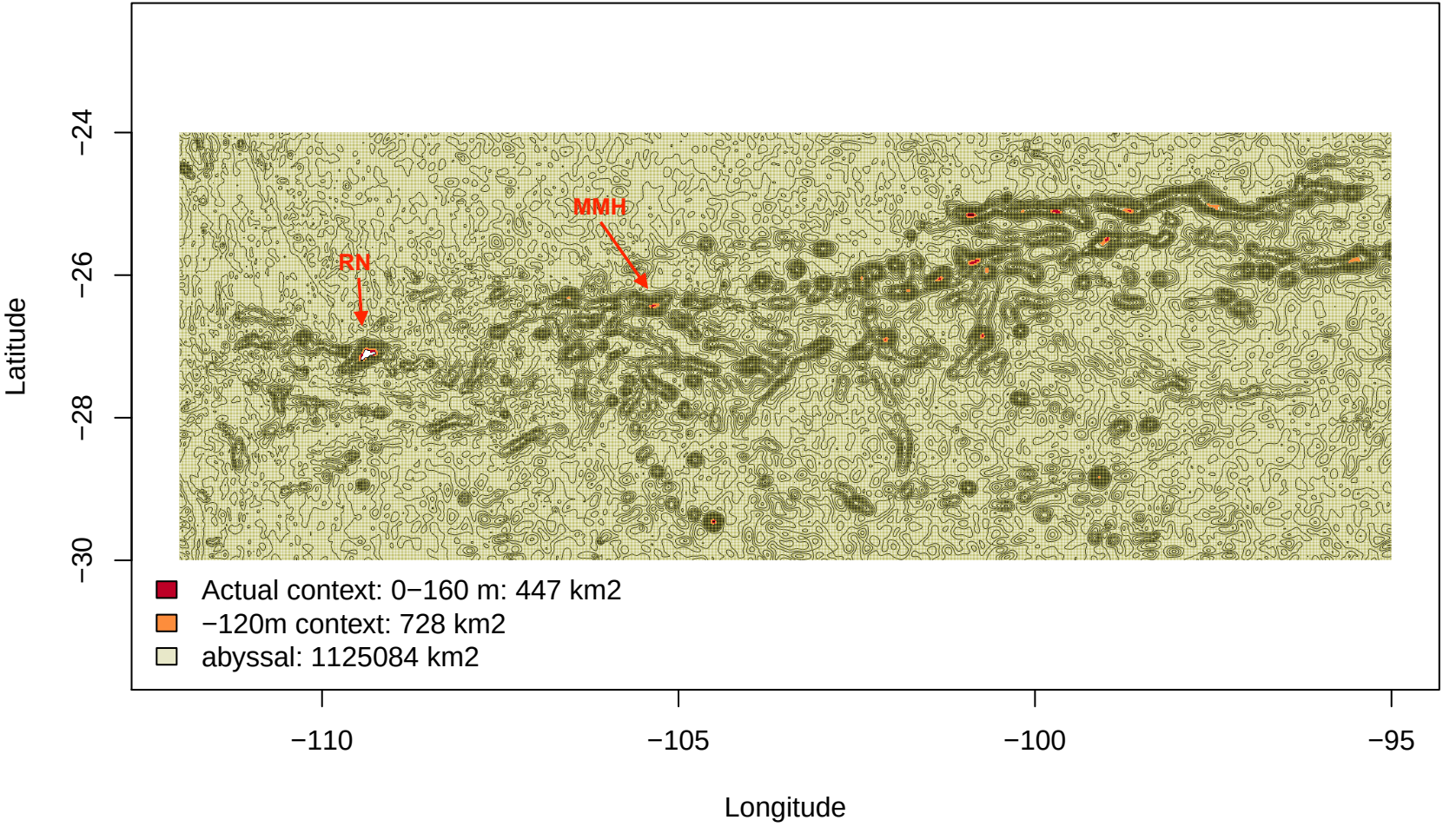
MMH
RN
Actual context: 0−160 m: 447 km2
−120m context: 728 km2
abyssal: 1125084 km2
−24
−26
−28
−30
Latitude
−110
−105
−100
−95
Longitude